



# Thermomechanical Property Prediction of Amorphous and Crystal PEKK via Molecular Dynamics

*Josh Kemppainen*  
*Michigan Technological University, Houghton, Michigan*

*Vikas Varshney*  
*Air Force Research Laboratory, Dayton, Ohio*

*Evan Pineda*  
*Glenn Research Center, Cleveland, Ohio*

*Gregory Odegard*  
*Michigan Technological University, Houghton, Michigan*

## NASA STI Program . . . in Profile

Since its founding, NASA has been dedicated to the advancement of aeronautics and space science. The NASA Scientific and Technical Information (STI) Program plays a key part in helping NASA maintain this important role.

The NASA STI Program operates under the auspices of the Agency Chief Information Officer. It collects, organizes, provides for archiving, and disseminates NASA's STI. The NASA STI Program provides access to the NASA Technical Report Server—Registered (NTRS Reg) and NASA Technical Report Server—Public (NTRS) thus providing one of the largest collections of aeronautical and space science STI in the world. Results are published in both non-NASA channels and by NASA in the NASA STI Report Series, which includes the following report types:

- **TECHNICAL PUBLICATION.** Reports of completed research or a major significant phase of research that present the results of NASA programs and include extensive data or theoretical analysis. Includes compilations of significant scientific and technical data and information deemed to be of continuing reference value. NASA counter-part of peer-reviewed formal professional papers, but has less stringent limitations on manuscript length and extent of graphic presentations.
- **TECHNICAL MEMORANDUM.** Scientific and technical findings that are preliminary or of specialized interest, e.g., “quick-release” reports, working papers, and bibliographies that contain minimal annotation. Does not contain extensive analysis.
- **CONTRACTOR REPORT.** Scientific and technical findings by NASA-sponsored contractors and grantees.
- **CONFERENCE PUBLICATION.** Collected papers from scientific and technical conferences, symposia, seminars, or other meetings sponsored or co-sponsored by NASA.
- **SPECIAL PUBLICATION.** Scientific, technical, or historical information from NASA programs, projects, and missions, often concerned with subjects having substantial public interest.
- **TECHNICAL TRANSLATION.** English-language translations of foreign scientific and technical material pertinent to NASA's mission.

For more information about the NASA STI program, see the following:

- Access the NASA STI program home page at <http://www.sti.nasa.gov>
- E-mail your question to [help@sti.nasa.gov](mailto:help@sti.nasa.gov)
- Fax your question to the NASA STI Information Desk at 757-864-6500
- Telephone the NASA STI Information Desk at 757-864-9658
- Write to:  
NASA STI Program  
Mail Stop 148  
NASA Langley Research Center  
Hampton, VA 23681-2199



# Thermomechanical Property Prediction of Amorphous and Crystal PEKK via Molecular Dynamics

*Josh Kemppainen*  
*Michigan Technological University, Houghton, Michigan*

*Vikas Varshney*  
*Air Force Research Laboratory, Dayton, Ohio*

*Evan Pineda*  
*Glenn Research Center, Cleveland, Ohio*

*Gregory Odegard*  
*Michigan Technological University, Houghton, Michigan*

National Aeronautics and  
Space Administration

Glenn Research Center  
Cleveland, Ohio 44135

## Acknowledgments

This research was conducted at NASA Glenn Research Center as a summer internship program and was supported by the NASA Glenn Thermoplastic Development for Exploration Applications (TDEA) program. SUPERIOR, a high-performance computing cluster at Michigan Technological University, was used in obtaining the MD simulation results presented in this publication.

Trade names and trademarks are used in this report for identification only. Their usage does not constitute an official endorsement, either expressed or implied, by the National Aeronautics and Space Administration.

*Level of Review:* This material has been technically reviewed by technical management.

# Thermomechanical Property Prediction of Amorphous and Crystal PEKK via Molecular Dynamics

Josh Kemppainen  
Michigan Technological University  
Houghton, Michigan 49931

Vikas Varshney  
Air Force Research Laboratory  
Dayton, Ohio 45431

Evan Pineda  
National Aeronautics and Space Administration  
Glenn Research Center  
Cleveland, Ohio 44135

Gregory Odegard  
Michigan Technological University  
Houghton, Michigan 49931

## Abstract

Traditionally, advanced aerospace composites have been manufactured using thermoset resins. However, recently, thermoplastics have been investigated for use in the manufacturing of composite materials due to their unique manufacturing characteristics. Thermoplastic resins can be reshaped and formed, along with the added benefit of being recyclable, which thermoset resin cannot. Thermoplastic materials undergo a crystallization process during manufacturing which affects the percent crystallinity of the material. The crystallization needs to be understood better to maximize the potential of thermoplastic resins. PEKK is a thermoplastic material with good chemical, thermal, and mechanical loading resistance. PEKK is also a material NASA is interested in for developing new bonded joint technology. The crystalline microstructure of PEKK is at the micrometer length scale, and it is of interest to model the effects of the crystallinity structure on PEKK's bulk properties. Molecular dynamics (MD) is a simulation tool that allows for property-structure relationships between atomistic structure and nanometer-length portions of a material. This makes MD a useful tool for developing the structure-property relationship of PEKK. However, the micrometer length scale of PEKK's crystal structure is too large for MD. Thus, a hybrid approach to modeling PEKK's microstructure is proposed in this work where MD models are built of both the amorphous and crystalline phases of PEKK. The engineering material properties can be obtained using MD at the nanometer length scale. A micromechanics approach can then generate the micrometer length scale of the crystallinity and the effective properties can be homogenized. The objective of this paper is to show the MD model workflow and the MD-predicted properties of PEKK. The properties can then be homogenized with different crystalline percentages to build design graphs that can be used to tailor PEKK for specific composite applications.

## Nomenclature

PEAK	Poly aryl ether ketone
PEKK	Poly ether ketone ketone
PEEK	Poly ether ether ketone
PMC	Polymer matrix composite
DPE	Diphenyl ether
I	Terephthalic acid
T	Isophthalic acid
MD	Molecular Dynamics
$\alpha$	Coefficient of thermal expansion
T <sub>g</sub>	Glass transition temperature

### 1.0 Introduction

PEKK (poly ether ketone ketone) belongs to the PAEK (poly aryl ether ketone) family of semi-crystalline thermoplastics. Semi-crystalline PAEK materials are known for their high performance in mechanical and thermal loading along with good chemical resistance (Ref. 1). Traditionally, polymer matrix composites (PMCs) have been manufactured using thermoset resins; however, recently thermoplastics have been investigated/used in PMC manufacturing due to their unique manufacturing characteristics and good properties. Thermoplastic materials can be reheated and reshaped several times with minimal to no degradation of properties.

A thermoplastic resin is received with all chemical reactions completed, and thus there are few manufacturing processes such as heating, cooling, and pressure which only affect the relaxation of molecular chains and crystallinity and not the chemistry of the material. This makes the challenges of specific processing conditions that affect the chemistry less complex than that of thermoset resins and ideal for use in advanced aerospace composites. Moreover, during the manufacturing of thermoset PMCs, residual stresses can occur due to a mismatch in the coefficient of thermal expansion between the matrix and the fiber and due to the matrix shrinkage caused by covalent bond formation. However, thermoplastic PMCs have near zero linear shrinkage since there are no covalent bonds forming during the processing of the bulk material. The crystallization process involves the densification of amorphous regions of the bulk material into crystalline form, which will produce localized shrinkage. The effects of localized shrinkage due to crystallization are not fully understood in the current literature. Further research into the characterization of this unique shrinkage of thermoplastic resin can help produce a more tailorable composite material.

What differentiates PAEK materials from one another is the ether/ketone ratio. PEEK is the most common PAEK material. PEEK has two ether bridges and one ketone between aryl groups, whereas PEKK has one ether bridge and two ketone bridges between aryl groups (Figure 1). The higher ketone percentage makes PEKK have a lower processing temperature as compared to PEEK. PEKK production starts with the reaction between diphenyl ether (DPE), terephthalic acid (T), and isophthalic acid (I) (Figure 2). By varying the quantities of terephthalic acid and isophthalic acid, PEKK can be polymerized into different structures having different T/I ratios. Different T/I ratios affect the crystallization kinetics which makes PEKK a tunable thermoplastic resin (Ref. 1). Arkema currently provides a wide range of T/I ratio bulk PEKK materials and it has been identified that Arkema's 7002 series (T/I 70/30) is of interest to the author (Ref. 1).

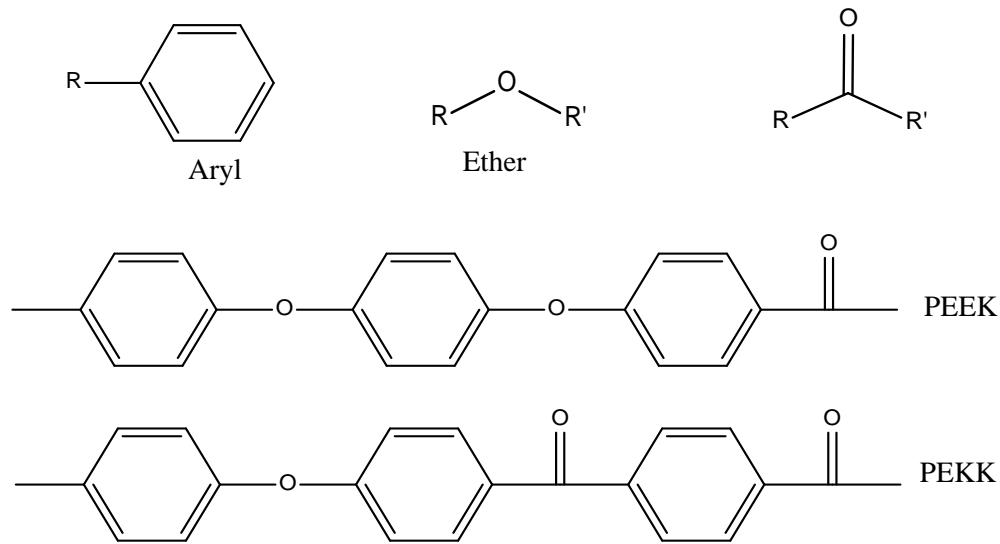


Figure 1.—PEKK and the PAEK family. PEKK and how it compares to PEEK.

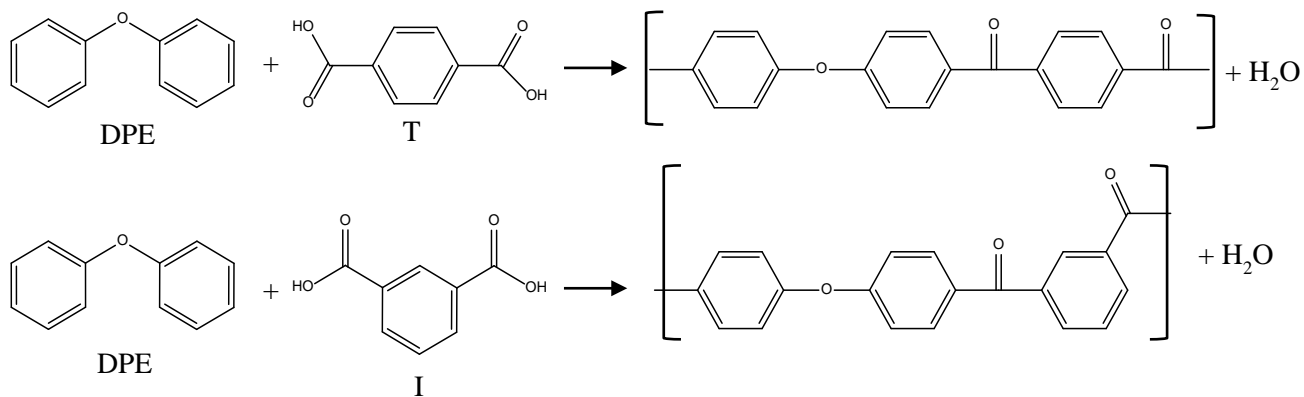


Figure 2.—PEKK chemical reactions. PEKK production by polymerizing diphenyl ether (DPE) with terephthalic acid (T) or isophthalic acid (I).

The microstructure of PEKK is a combination of amorphous and crystalline phases. The amount of crystalline phase present in the final material is dependent on T/I ratios and processing parameters. The crystallization produces microstructures called spherulites which are comprised of plank-like semicrystalline structures surrounded by amorphous regions that spread out in a radial manner (Figure 3). The plank-like structures are comprised of crystal lamella (Figure 4). There are three crystal forms of pure PEKK with different crystalline unit cells and lattice constants (Figure 5).

Molecular Dynamics (MD) is a modeling technique that explicitly models the atoms with empirically derived forcefields. There are a variety of different forcefields available, however, IFF/IFF-R (Interface force field/Reactive interface force field) has been shown to predict polymer properties very well (Ref. 4). IFF was a reparameterization of PCFF (Polymer consistent force field) (Ref. 5) of the nonbonded interactions and IFF-R introduced bond scissions via the inclusion of a morse bonding parameter. Some other MD work was carried out on PEKK using the Deriding united atom forcefield by Li et al. to predict thermophysical properties (Ref. 6). No mechanical properties of PEKK were computed by Li et al. To the author's knowledge, no other MD work has been done on the mechanical properties of PEKK. It is then desired to develop MD models of PEKK to determine the thermomechanical properties of PEKK using the IFF/IFF-R forcefield.

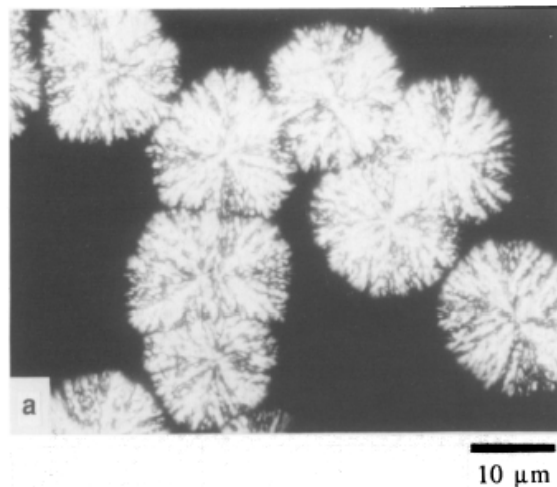


Figure 3.—PEKK microstructure of spherulite crystals embedded in amorphous regions. Polarized microscopic image of spherulite (Ref. 2).

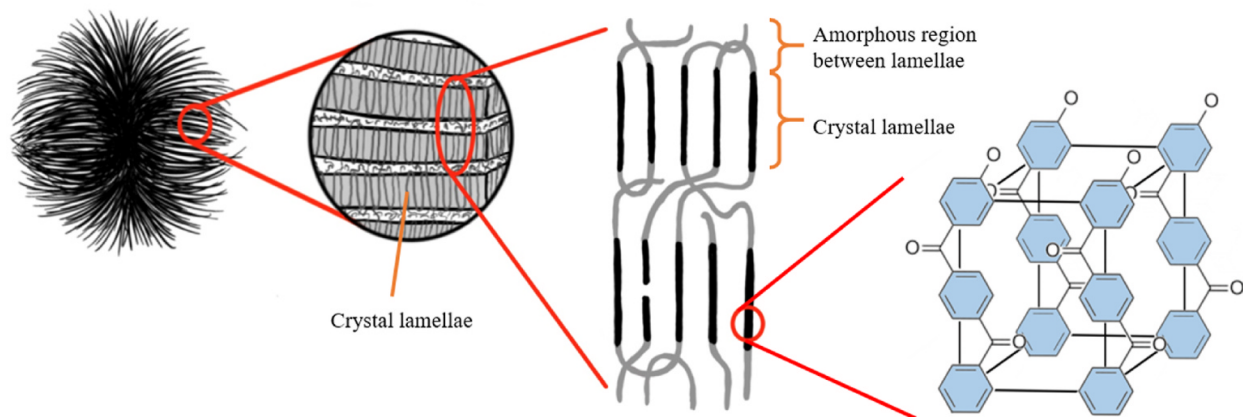


Figure 4.—Spherulite compositions. The length scale decreases from left to right as the micrometer length scale gets decomposed to the nanometer length scale (Ref. 1).

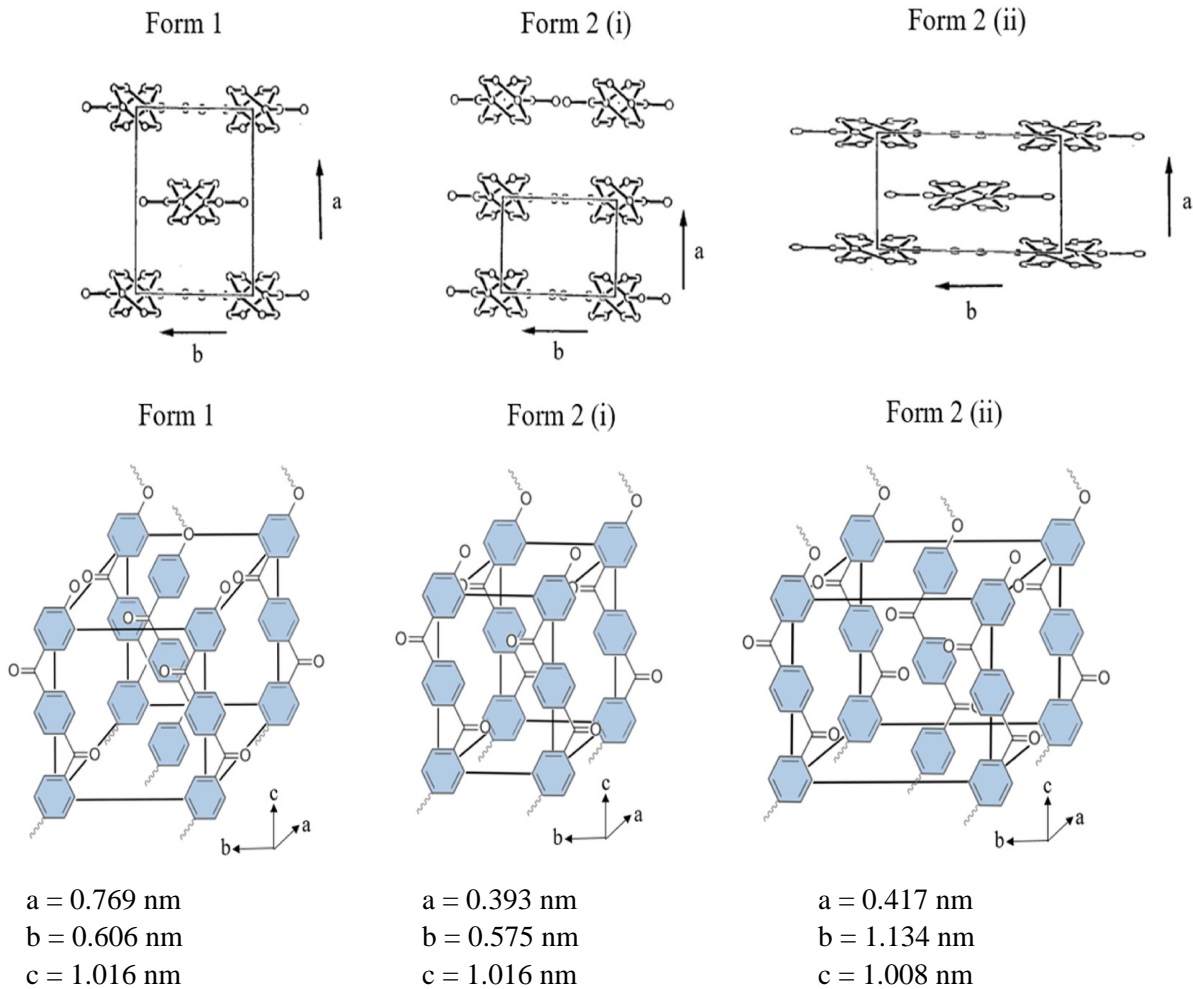


Figure 5.—PEKK crystalline unit cells. Form 1 is two chain orthorhombic, Form 2i is one chain orthorhombic proposed by Gardner et al. (Ref. 2), and Form 2ii is two chain orthorhombic purposed by Blundell et al. (Ref. 3).

MD is computationally limited to the nanosecond time scale and nanometer length scale, whereas PEKK is a multiscale from the nanometer length to the micrometer length scale. Thus, the length scale size of PEKK's microstructure is outside of what MD can do. A multiscale micromechanics approach is needed to homogenize the MD properties to the microscale spherulite as Pisani et al. have done with PEEK (Ref. 7). This approach will require specific MD modeling of the amorphous and crystalline phases of PEKK which are nanoscale in nature and then homogenizing the microscale. The objective of this paper is to show the workflow used to generate the MD properties of a T/I ratio of 70/30 PEKK (a material of interest to the NASA Thermoplastic Development for Exploration Applications (TDEA) program). Future work will homogenize the spherulitic microstructure using multiscale recursive micromechanics to predict bulk properties of PEKK as a function of crystallinity (Ref. 8).

## 2.0 Molecular Dynamics Model Building Workflow

All MD simulations were carried out using the LAMMPS June 23, 2022, version. All MD model's topologies were built in Chemdraw 21.0.0 and were minimized with an RMS minimum gradient of 0.001. The topological files were then exported, and an in-house python code was used to convert the file to a LAMMPS datafile and insert IFF parameters. All models were built in IFF and then converted to IFF-R for mechanical deformations. The standard class2 harmonic bonding potential of IFF was left as is for thermal simulations since bond scission is not expected during thermal simulations and the bond scission capabilities in IFF-R require lower timestep values to absorb the energy released during a bond scission event. The PEKK system of interest is Arkema's 7002 series, which has a T/I ratio of 70/30, so all MD models will be built to have a T/I ratio of 70/30. The starting molecules for all simulations of PEKK are pre-polymerized diphenyl ether with terephthalic acid (DPET) and diphenyl ether with isophthalic acid (DPEI) (Figure 6).

### 2.1 Amorphous PEKK MD Models

For the amorphous MD models, the starting molecules were first mixed in a 7:1 ratio DPET to DPEI to create the T/I ratio of 70/30 at 300 K in the NVT ensemble for 100 ps. Two different types of simulation cells are desired for the property's prediction (mechanical vs. thermal properties), (1) an orthogonal cubic cell and (2) an orthogonal cuboid cell. The mixed molecules were then replicated N-number of times in each direction to build model sizes of 18,240 atoms (cubic cell) and 19,760 (cuboid cell) atoms using LAMMPS's replicate command. The number of atoms in the cubic cell and cuboid cell were matched as close as possible, but due to the difference in simulation cell size, the cuboid cell has about 1500 more atoms than the cubic cell system. After replication, the simulation cells were then deformed using LAMMPS's deform command at 300 K in the NVT ensemble for 4 ns until the cubic and cuboid shapes' density was 1.29 g/cm<sup>3</sup> (the density of bulk PEKK) (Ref. 9). The molecules were then reacted with one another by building bond/react templates that polymerize in the fashion of Figure 2, leaving water as the by-product (Ref. 10). A maximum distance of bonding initiator atom ids of 6 angstroms was used and a bonding probability of 0.5 was used. The inter molecule flag was also utilized to make sure there was no cyclization of PEKK chains. The conversion factor was computed using Equation (1), where  $N_0$  is the number of initial starting molecules and  $N$  is the number of final molecules in

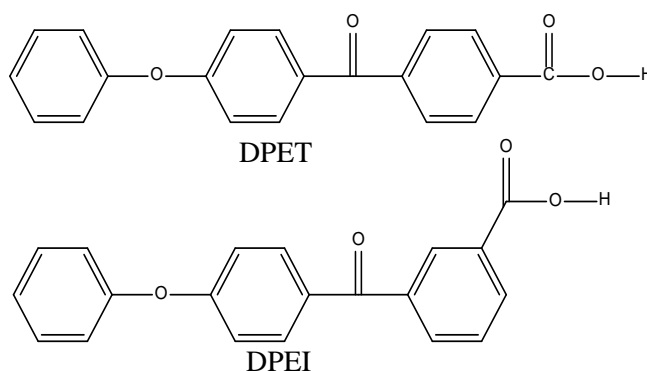


Figure 6.—MD Starting molecules. DPET is the MD starting molecule for the diphenyl ether + terephthalic acid moieties and DPEI is the MD starting molecule for the diphenyl ether + isophthalic acid moieties.

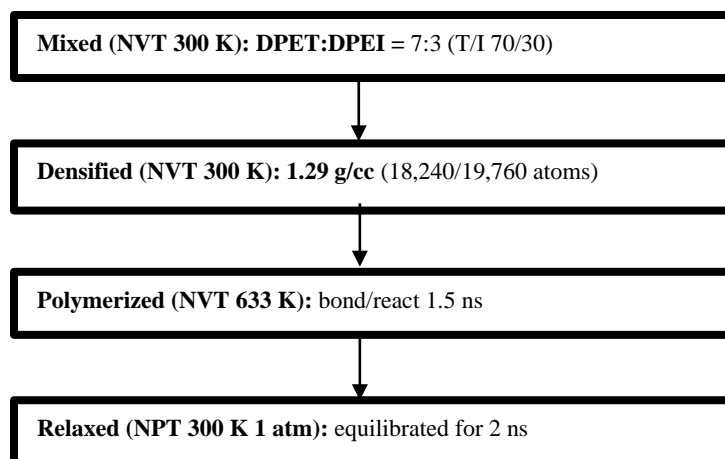


Figure 7.—MD amorphous model building workflow. All amorphous MD models were built in this sequence.

the system and is meant to model simple polycondensation reactions like what occur for PEKK polymerization (Ref. 11). The water molecules were deleted after each reaction and the conversion factor was found to be converged after 1.5 ns setting the endpoint of polymerization. The temperature used during polymerization was 633 K, the processing temperature of Arkema’s PEKK 7002 series (Ref. 9). The polymerized models were then equilibrated at 300 K 1 atm using the NPT ensemble. A workflow of the modeling building process can be seen in Figure 7. Five replicates were built by changing the velocity seed at the mixing, densifying, and polymerization steps to create different morphologies.

$$p = \frac{N_o - N}{N_o} \quad (1)$$

## 2.2 Crystal PEKK MD Models

For the crystal MD models, the starting molecules were read in one above another in the z-direction to establish the simulation cell as the long dimension in the z-direction in a 7:1 ratio DPET to DPEI. The DPEI moieties were randomly distributed throughout the DPET moieties during the reading in stage. The molecules were then reacted with one another by using the same bond/react templates that were used in the amorphous modeling building stage. A maximum distance of bonding initiator atom ids of 10 angstroms was used and a bonding probability of 0.5 was used at 633 K. The inter molecule flag was also utilized to make sure there was no cyclization of PEKK chains and water by products were removed after each reaction. This was run for 10 ps until 9 reactions were observed. Next, the polymerized chain of 10 starting molecules was subjected to 1000 K and 1000 atm with anisotropic settings to allow the chain to straighten out in the NPT ensemble. The last stage in making the building block of all crystalline unit cells was to react the molecule along the z-direction to be bonded periodically, and this was done using bond/react with the intra molecule flag followed by a 1 ns 300 K 1 atm NPT equilibration. The evolution of this process can be seen in Figure 8.

The starting chain of PEKK T/I ratio 70/30 has now been built and is ready to insert into the specific crystalline unit cell of Form 1, Form 2i, and Form 2ii. Form 1 is a two-chain orthorhombic cell. To make this unit cell, the linear chain created was replicated in the x-direction by a factor of 2 and then the simulation cell dimensions were deformed to the experimental dimensions seen in Figure 5. Form 2i is a one-chain orthorhombic cell. To make this unit cell, the linear chain created was not replicated, and then

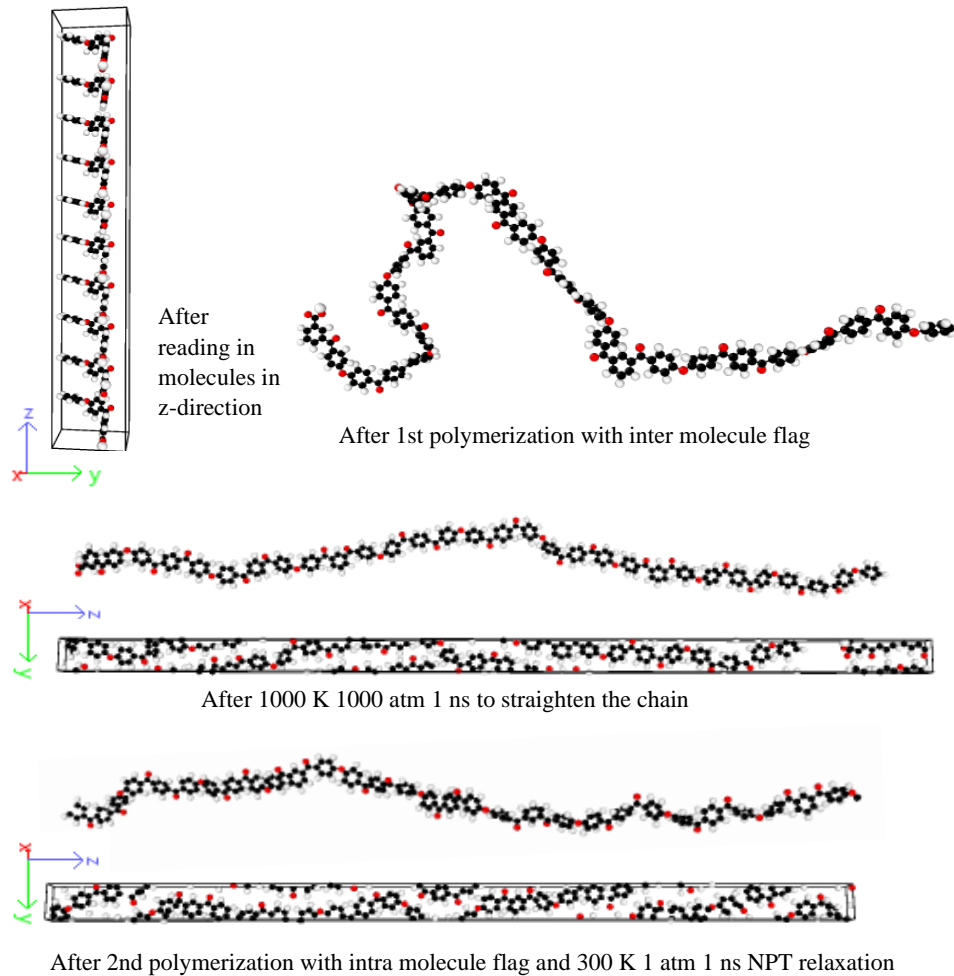


Figure 8.—MD crystal building block chain building workflow. Steps increase from left to right and top down.

the simulation cell dimensions were deformed to the experimental dimensions seen in Figure 5. Form 2ii is a two-chain orthorhombic cell. To make this unit cell, the linear chain created was replicated in the y-direction by a factor of 2 and then the simulation cell dimensions were deformed to the experimental dimensions seen in Figure 5.

Thus, a-direction in each unit cell corresponds to x-direction in LAMMPS, b-direction corresponds to y-direction in LAMMPS, and c-direction corresponds to z-direction in LAMMPS. Each unit cell was then replicated minimally in each direction such that the dimension of the simulation cell was larger than 10 angstroms. The purpose of this is because the Leonard-Jones Van der Waals cut-off used was 10 angstroms, and now all Van der Waal interaction will occur inside the supercell or in the 1st images of the supercell. LAMMPS uses the minimum image convention of the Leonard-Jones cutoff so all Van der Waal interactions will now be accounted for in the unit cell and its 1st images. Lastly the model was equilibrated at 300 K and 1 atm for 2 ns using the NPT ensemble. The entire crystalline building workflow can be seen in Figure 9 and process of making the linear molecule into crystalline unit cells and then the replication of the unit cell to a supercell can be seen in Figure 10.

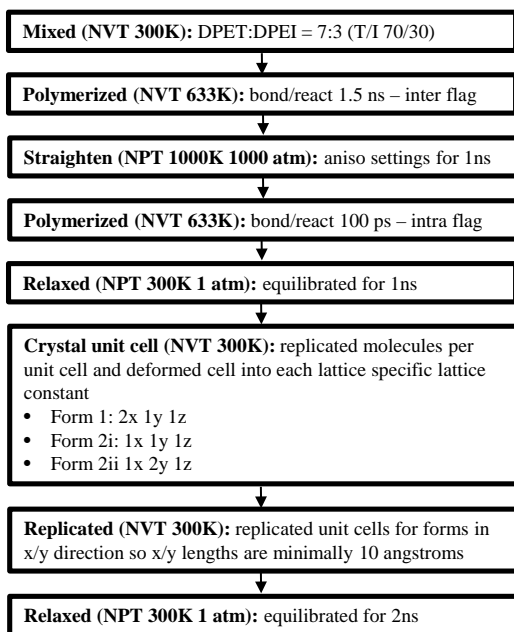


Figure 9.—MD crystal model building workflow. All crystal MD models were built in this sequence.

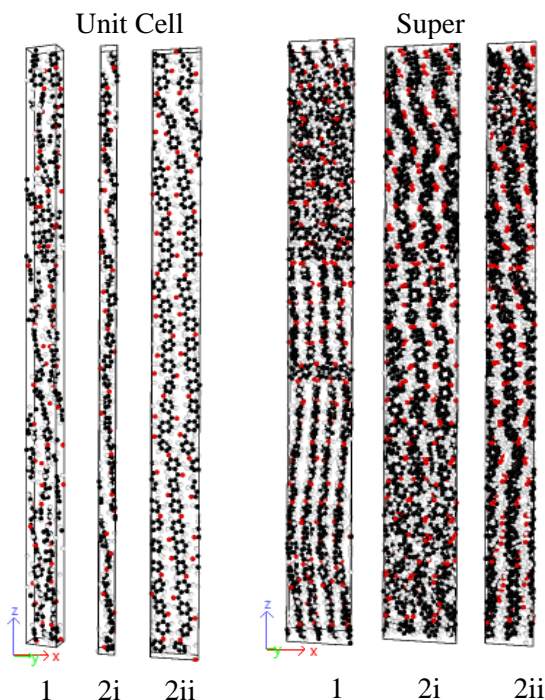


Figure 10.—MD crystal unit cell/super cell building workflow. Steps increase from left to right.

### 3.0 Molecular Dynamic Property Simulations

#### 3.1 Mechanical Properties

During all mechanical property's simulation, IFF-R was used to allow bond scission via the morse bonding potential. Tensile and Shear simulations were carried out on all models with a tensile strain rate of  $1 \times 10^8 S^{-1}$  and a shear strain rate of  $2 \times 10^8 S^{-1}$ . The strain rates applied are larger than what are performed at the macros scale, thus the computed MD elastic moduli are typically over predicted as compared to macro level material properties. The amount of over prediction of the MD model typically is dependent on the viscoelastic nature of the specific system. This means that the crystalline MD models will observe less of strain rate effect than its amorphous counter parts. During all mechanical simulations, the NPT ensemble was used at 300 K and 1 atm which allowed for the poison's contraction of the tensile simulations. The tensile simulations were used to determine the elastic modulus, nonlinear modulus, tensile strength, and Poisson's ratio. During tensile straining, the amorphous system undergoes chain unwrapping which creates a multistage elastic modulus after the unwrapping. The 1st linear slope of the stress-strain data is taken to be the elastic modulus of the material, and the break point of the 1st linear region is taken to be the tensile yield strength. After the first unwrapping of chains, the amorphous material can sustain more load until the next polymer chain unwraps again, and this gives rise to a secondary tensile modulus. This secondary tensile modulus is taken to be the nonlinear modulus of the amorphous material (Figure 11). After the secondary modulus, there were no other observable stiffnesses (slopes of stress-strain data) of the system. Meaning that the system was strained enough that the model could not sustain load reliably. The shear simulations were used to determine the shear modulus and shear yield strength. Where the shear modulus and shear yield strength were found by the same methods used for tensile simulations.

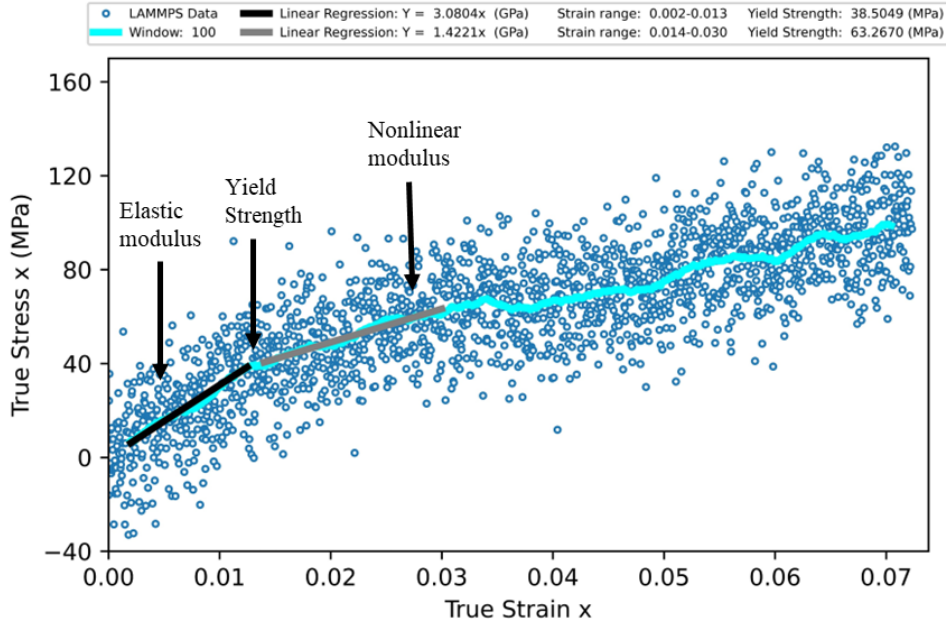


Figure 11.—Representative stress-strain curve. With Elastic modulus, yield strength and nonlinear modulus shown.

### 3.2 Thermal Properties

For the thermal property’s simulations, IFF was used for its computational efficiency for both the amorphous and crystalline phases. Cubic models were used to compute coefficient of thermal expansion ( $\alpha$ ) and glass transition temperature ( $T_g$ ). The simulation used a temperature ramp from 100 to 750 K for the heating simulation and 750 to 100 K for the cooling simulation. A heating/cooling rate of 50 K/ns was used for all temperature sweeps. The density and volume were logged and the  $\alpha$  below  $T_g$  is computed from the volume-temperature slope ( $dV/dT$ ) below  $T_g$  and  $\alpha$  above  $T_g$  is computed from the volume-temperature slope ( $dV/dT$ ) above  $T_g$  using where the volume ( $V$ ) is the room temperature volume of the simulation Equation (2) (Figure 12).

Thermal conductivity was computed using the cuboid models and the direct method. The direct method involves building a cuboid simulation cell so a spatial temperature gradient can be accurately computed. The cuboid cell in the long direction ( $z$ -directions for all models) is 208 angstroms for amorphous systems and 150 angstroms for crystalline systems and is then decomposed into regions (Figure 13). The two fixed end regions are to allow for heat transfer in one direction and were 10 angstroms long. The dimension of 10 angstroms was chosen because the Van der Waals cut-off used was 10 angstroms and this would make sure no Van der Waals interaction would occur across the periodic boundaries. Next to the fixed regions, two other regions were defined to apply thermostats. These regions were 20 angstroms in length, and the hot thermostat was set to 350 K, and the cold was set to 250 K. The center region was time integrated to transfer the heat from one thermostat to the other.

$$a = \frac{1}{3v} \left( \frac{dV}{dT} \right) \quad (2)$$

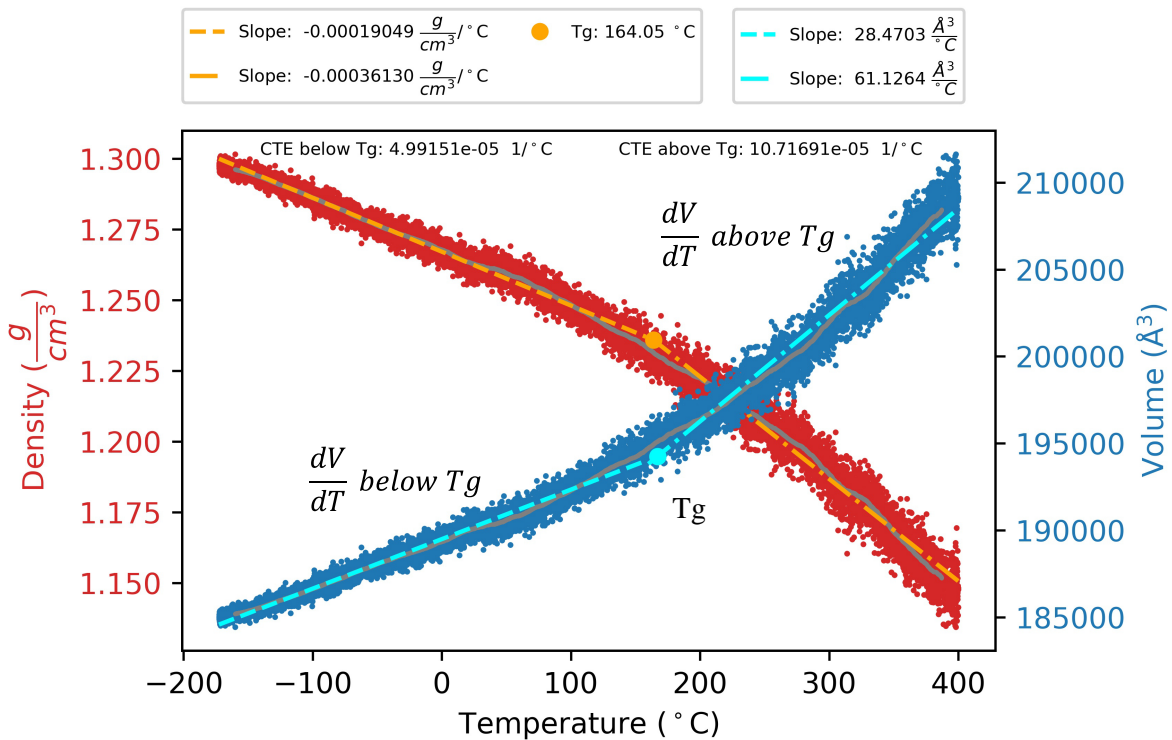


Figure 12.—Representative volume/density-temperature curve. With  $T_g$  shown as the bi-linear break point and the  $dV/dT$  slopes shown for CTE calculation.

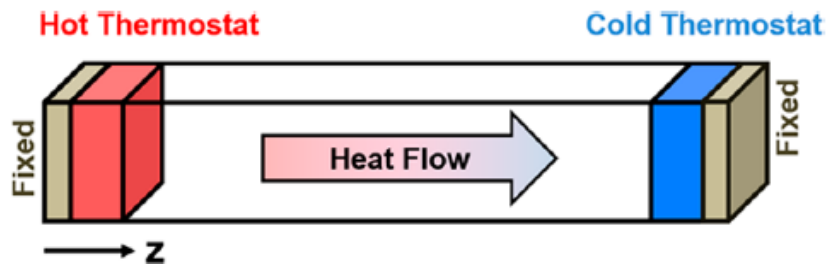


Figure 13.—Cuboid regions for thermal conductivity calculations. Regions of the cuboid simulation cell. Image from (Ref. 12).

Thermal conductivity ( $K$ ) was computed using Equation (3), where the numerator is the heat flux across the simulation cell, and the denominator is the spatial temperature gradient across the center region of the simulation cell (Ref. 12).

$$K = \frac{\frac{Q}{A \Delta t}}{\frac{dT}{dz}} \quad (3)$$

The heat flux, or numerator of Equation (3), is composed of  $Q$  being the heat energy,  $A$  is the cross-sectional area, and  $\Delta t$  is the change in simulation time. The spatial temperature gradient, or denominator of Equation (3), is composed of the  $dT/dz$  which is computed from the temperature profile in the center region (Figure 14).

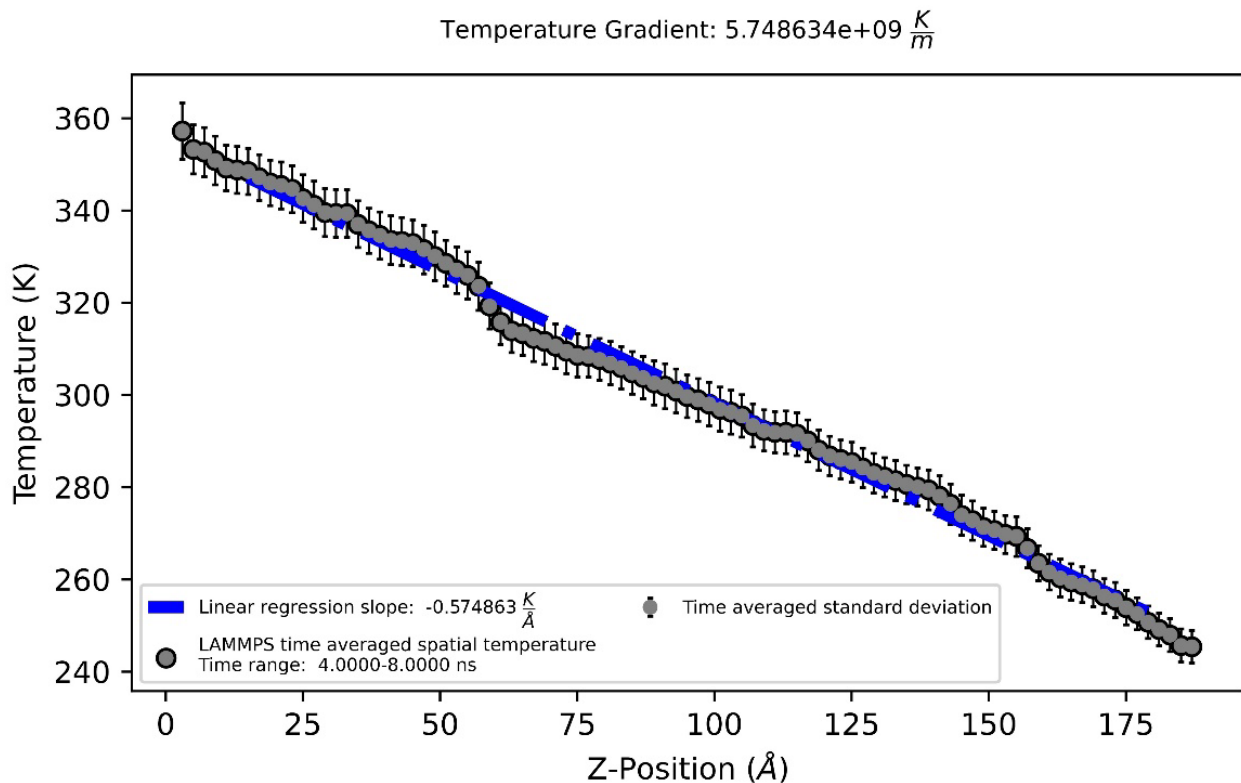


Figure 14.—Representative temperature profile curve. The slope of the curve is computed with a linear regression model and is the spatial temperature gradient.

## 4.0 Results and Discussion

All properties were obtained by methods explained in the simulation sections. The mechanical properties of the amorphous and crystalline system can be found in Table I. The amorphous system is isotropic, so all mechanical properties obtained from all five replicates in each direction were averaged together and the standard deviation was used for the tolerance. There were three forms of the crystalline system modeled and it is not fully known which of the forms exists for PEKK with a T/I ratio of 70/30. Due to this uncertainty of structures, all longitudinal (z-direction) properties were averaged together for all three forms, and all transverse properties (x-direction and y-direction) were averaged together and reported with the standard deviation as the tolerance of the properties. The individual mechanical properties for each crystalline form are also provided in Table II. Only one system of each form was modeled so no tolerances on mechanical properties are reported in Table II.

The thermal simulation properties can be found in Table III. The density is listed both in Table I, Table II, and Table III because density plays a large role in any MD properties. Aside from the differences in chain configuration, the biggest factor between the amorphous and crystalline properties will be the associated density of each model. For the amorphous thermal properties, all five replicate values were averaged over, and the standard deviation was given to show the tolerance. For the crystalline

TABLE I.—MECHANICAL PROPERTIES OF BOTH AVERAGE AMORPHOUS AND AVERAGE CRYSTALLINE PHASES OF MD MODEL

Property	Amorphous	Crystalline
Density (g/cm <sup>3</sup> )	1.2505±0.0043	1.3856±0.0183
E <sub>xx</sub> Linear (Gpa)	2.6108±0.5272	2.9603±0.7925
E <sub>yy</sub> Linear (Gpa)	2.6108±0.5272	2.9603±0.7925
E <sub>zz</sub> Linear (Gpa)	2.6108±0.5272	163.4538±2.0270
G <sub>xy</sub> (Gpa)	0.8423±0.0692	1.2724±0.4758
G <sub>xz</sub> (Gpa)	0.8423±0.0692	1.3769±0.6875
G <sub>yz</sub> (Gpa)	0.8423±0.0692	1.2174±0.4634
v <sub>xy</sub>	0.4398±0.0156	0.3199±0.0508
v <sub>xz</sub>	0.4398±0.0156	0.3199±0.0508
v <sub>yz</sub>	0.4398±0.0156	0.3199±0.0508
σ <sub>Ys XX</sub> (Mpa)	40.6491±10.7473	172.4277±39.3476
σ <sub>Ys YY</sub> (Mpa)	40.6491±10.7473	172.4277±39.3476
σ <sub>Ys ZZ</sub> (Mpa)	40.6491±10.7473	-----
τ <sub>xy</sub> (Mpa)	34.0689±7.1541	32.2045±8.6538
τ <sub>xz</sub> (Mpa)	34.0689±7.1541	32.2045±8.6538
τ <sub>yz</sub> (Mpa)	34.0689±7.1541	32.2045±8.6538
E <sub>xx</sub> nonlinear (Gpa)	2.0039±0.3125	-----
E <sub>yy</sub> nonlinear (Gpa)	2.0039±0.3125	-----
E <sub>zz</sub> nonlinear (Gpa)	2.0039±0.3125	-----

system all three forms were averaged over, and the standard deviation was given to show the tolerance. The CTE and Tg for both the amorphous and crystalline phases are the averages of the heating and cooling simulations.

The MD properties cannot be compared to literature/experimental values since all MD values are at the nanometer length scale, and all experimental values in the literature values are found at the macroscale. This means that all literature values of bulk PEKK T/I 70/30 are a combination of amorphous and crystalline phases organized into the spherulite structures of PEKK (Figure 4). The mass density of the crystalline forms can be compared to experimental density found by Blundell et al. of about 1.4 g/cc for an unknown T/I ratio PEKK crystalline phase (Ref. 3). The predicted mass density of modeled Form 1 and Form 2ii best match the experimental density of PEKK crystalline density reported by Blundell et al. (Table II). However, Form 2i is also within reason on predicted density since it is unknown the PEKK T/I ratio that Blundell et al. used. The Tg values computed herein can be compared to Li et al. MD models

TABLE II.—MECHANICAL PROPERTIES OF EACH MODELED CRYSTALLINE FORM

Property	Form 1	Form 2i	Form 2ii
Density (g/cm <sup>3</sup> )	1.3986	1.3647	1.3936
E <sub>xx</sub> Linear (Gpa)	3.9635	3.6257	4.8119
E <sub>yy</sub> Linear (Gpa)	2.9088	1.2932	1.1588
E <sub>zz</sub> Linear (Gpa)	163.7327	165.3269	161.3018
G <sub>xy</sub> (Gpa)	1.3296	1.7170	16.1817
G <sub>xz</sub> (Gpa)	0.6368	1.9957	49.4406
G <sub>yz</sub> (Gpa)	1.7514	0.9799	44.2031
v <sub>xy</sub>	0.4277	0.3316	0.3635
v <sub>xz</sub>	0.1890	0.2277	0.2979
v <sub>yz</sub>	0.1909	0.2534	0.2979
σ <sub>Ys XX</sub> (Mpa)	218.1571	228.4172	264.6519
σ <sub>Ys YY</sub> (Mpa)	170.4301	77.5908	75.3190
σ <sub>Ys ZZ</sub> (Mpa)	-----	-----	-----
τ <sub>xy</sub> (Mpa)	79.6197	17.1702	16.1817
τ <sub>xz</sub> (Mpa)	15.9125	29.9361	49.4406
τ <sub>yz</sub> (Mpa)	17.7794	19.5974	44.2031

TABLE III.—THERMAL PROPERTIES OF BOTH AMORPHOUS AND CRYSTALLINE PHASES OF MD MODEL

Property	Amorphous	Crystalline
Density (g/cm <sup>3</sup> )	1.2505±0.0043	1.3856±0.0183
CTE Below Tg (1/°C)	5.3348×10 <sup>-5</sup> ±8.5852×10 <sup>-7</sup>	5.6373×10 <sup>-5</sup> ±3.6761×10 <sup>-6</sup>
CTE Above Tg (1/°C)	11.2736×10 <sup>-5</sup> ±6.8894×10 <sup>-6</sup>	8.5020×10 <sup>-5</sup> ±1.1443×10 <sup>-5</sup>
Tg (°C)	164.0314±3.5787	207.1828±1.4262
Thermal Conductivity (W/(m-K))	0.4298±0.1719	2.7950±0.2119

using the Dreiding force field, where they modeled different T/I ratio models of PEKK that were a combination of amorphous and crystalline phases and found out at the nanometer length a combination of amorphous and crystalline phases of PEKK produced a T<sub>g</sub> value between 196 to 206 °C (Ref. 6). Comparing this value to my pure crystal models shows that my crystal models are close to what Li et al. had found with their work (Table III). The amorphous models can then be implied that the T<sub>g</sub> matches well for what they are, since it is not truly known the crystallinity percent of the MD models built by Li et al. To the authors knowledge no other computed properties can be compared to other work researchers work since the current literature is sparse on PEKK's nanometer length scale properties.

Future work will need to be done to homogenize the properties of the nanometer length scale MD results to be able to compare to macroscale experimental data in the literature. The homogenization will be done in a similar way as Pisani et al. did with the Micromechanics Analysis Code/Generalized Method of Cells (MAC/GMC), developed at the NASA Glenn Research Center (GRC), but with new micromechanics code called the NASA Multiscale Analysis Tool (NASMAT, also developed at GRC) (Refs. 7 and 8). During the homogenization of the MD properties, different ratios of amorphous and crystalline phases can be mixed to build design graphs showing the effective properties of that specific percent crystallinity. The design graphs then can be used to tailor PEKK for specific aerospace composite applications.

## 5.0 Conclusion

PEKK is a thermoplastic material that belongs to the PAEK family and has two distinct microstructures of amorphous and crystalline phases making PEKK's microstructures a multiscale problem. PEKK also is tunable in terms of T/I ratios and the T/I ratio of interest is that of 70/30. PEKK crystal phases have three unique possible forms of Form 1, Form 2i, and Form 2ii. The three crystalline forms lattice constants were for pure PEKK of a T/I ratio of 100/0. It is unknown to the author what the exact crystalline unit cells are for PEKK T/I ratio of 70/30. Molecular dynamics models of PEKK were built for both the amorphous and crystalline phases with a T/I ratio of 70/30. Five replicates of amorphous were built and each of the three forms of crystalline phase were built for the crystalline models. The three forms of crystalline phases were built in as the three known forms of pure PEKK, but then the force-field used set the final crystalline lattice constants. Thermomechanical properties were determined for both the crystalline and amorphous phases. The properties are at the nanometer length scale and PEKK's microstructure is at the micrometer length scale. Future work will be performed to homogenize the amorphous and crystalline phases of PEKK together with different quantities of crystalline/amorphous phases to generate build design graphs of what type of properties are expected of PEKK based on crystallinity percent. The design graphs will act as a guide for designing the PEKK material desired to use in advanced aerospace composites.

## References

1. Pérez-Martín, H., Mackenzie, P., Baidak, A., Ó Brádaigh, C.M., and Ray, D., "Crystallinity studies of Pekk and Carbon Fibre/Pekk Composites: A Review," *Composites Part B: Engineering*, vol. 223, 2021, pp. 109–127.
2. Gardner, K.C.H., Hsiao, B.S., Matheson, R.R., and Wood, B.A., "Structure, crystallization and morphology of poly (aryl ether ketone ketone)," *Polymer*, vol. 33, 1992, pp. 2483–2495.
3. Blundell, D.J., and Newton, A.B., "Variations in the crystal lattice of peek and related para-substituted aromatic polymers: 2. effect of sequence and proportion of ether and ketone links," *Polymer*, vol. 32, 1991, pp. 308–313.

4. Winetrout, J.J., Kanhaiya, K., Sachdeva, G., Ravindra Pandey, R., Adri van Duin, A., Gregory Odegard, G., and Heinz, H., “Implementing Reactivity in Molecular Dynamics Simulations with the Interface Force Field (IFF-R) and Other Harmonic Force Fields,” *preprint arXiv:2107.14418*, 2021.
5. Sun, H., Mumby, S.J., Maple, J.R., and Hagler, A.T., “An ab initio CFF93 all-atom force field for polycarbonates,” *Journal of the American Chemical Society*, vol. 116, 1994, pp. 2978–2987.
6. Li, C., and Strachan, A., “Prediction of PEKK properties related to crystallization by molecular dynamics simulations with a united-atom model,” *Polymer*, vol. 174, 2019, pp. 25–32.
7. Pisani, W.A., Radue, M.S., Chinkanjanarot, S., Bednarcyk, B.A., Pineda, E.J., Waters, K., Pandeya, R., King, J.A., and Odegard, G.M., “Multiscale modeling of peek using reactive molecular dynamics and Micromechanics,” *American Society for Composites 2017*, 2017, pp. 96–105.
8. Pineda, E.J., Ricks, T.M., Bednarcyk, B.A., and Arnold, S.M., “Benchmarking and performance of the NASA multiscale analysis tool,” *AIAA Scitech 2021 Forum*, 2021.
9. “Kepstan 7002 Datasheet,” CAMPUSplastics Available: <https://www.campusplastics.com/campus/en/datasheet/Kepstan%C2%AE+7002/ARKEMA/179/3e832658>.
10. Gissinger, J.R., Jensen, B.D., and Wise, K.E., “Modeling chemical reactions in classical molecular dynamics simulations,” *Polymer*, vol. 128, 2017, pp. 211–217.
11. Cowie, C.J.M., and Arrighi, V., *Polymers: Chemistry and physics of modern materials*, Boca Raton, FL: CRC/Taylor & Francis, 2008.
12. Radue, M.S., Varshney, V., Baur, J.W., Roy, A.K., and Odegard, G.M., “Molecular modeling of cross-linked polymers with Complex Cure Pathways: A case study of bismaleimide resins,” *Macromolecules*, 2018, pp. 1830–1840.



